Global QBO Circulation Derived from UKMO Stratospheric Analyses

WILLIAM J. RANDEL AND FEI WU

Atmospheric Chemistry Division, National Center for Atmospheric Research, Boulder, Colorado

RICHARD SWINBANK AND JOHN NASH

U.K. Meteorological Office, Bracknell, Berkshire, United Kingdom

ALAN O'NEILL

Centre for Global Atmospheric Modelling, Department of Meteorology, University of Reading, Reading, United Kingdom

(Manuscript received 11 July 1997, in final form 31 March 1998)

ABSTRACT

Global circulation anomalies associated with the stratospheric quasi-biennial oscillation (QBO) are analyzed based on U.K. Meteorological Office (UKMO) assimilated wind and temperature fields. Zonal winds and temperatures from the assimilation are compared with Singapore rawinsonde data (the standard QBO reference time series), showing reasonable agreement but an underestimate of maxima in the UKMO analyses. Global structure of the QBO in zonal wind, temperature, and residual mean meridional circulation (derived from thermodynamic balance and mass continuity) is isolated, showing coherent tropical and midlatitude components. Important aspects of the QBO revealed in these data include 1) out of phase maxima in temperature (and vertical velocity) between the lower and upper stratosphere, and 2) strong seasonal synchronization of midlatitude anomalies. These characteristics are also evident in long records of satellite radiance measurements.

1. Introduction

Interannual variability of zonal winds and temperatures in the tropical stratosphere is dominated by an approximate 2-year periodicity termed the quasi-biennial oscillation (QBO). The QBO was discovered independently by Reed et al. (1961) and Veryard and Ebdon (1961). Characteristics of the QBO in tropical zonal winds and temperatures have been derived from long time series of rawinsonde observations by Angell and Korshover (1962), Hamilton (1984), Dunkerton and Delisi (1985), and Naujokat (1986). Satellite-based wind observations show a QBO structure in reasonable agreement with rawinsonde observations (Ortland et al. 1996), but temporal and altitude coverage is limited. Satellite temperature measurements are useful for isolating temporal variations and latitudinal structure of the QBO (e.g., Nash 1988; Christy and Drouilhet 1994), but because of the narrow vertical structure of QBO temperature anomalies, temperatures and balanced winds derived from nadir-sounding satellite instruments substantially underestimate QBO amplitudes (e.g., Fleming and Chandra 1989). Improved global characterization of the QBO is possible using data assimilation techniques, which optimally combine satellite and radiosonde measurements into a global analysis, using an atmospheric general circulation model. The focus of this work is to analyze the global space–time character of the QBO using output of the United Kingdom Meteorological Office (UKMO) stratospheric assimilation (Swinbank and O'Neill 1994a). The ability of the UKMO assimilation to capture tropical zonal wind QBO variations was shown in Swinbank and O'Neill (1994b). Here we look in more detail at QBO circulation anomalies in the UKMO data, based on the time period November 1991–October 1998 (almost three complete QBO cycles).

There are two main aspects to this paper. First, we make systematic comparisons between the UKMO analyses of zonal winds and temperatures and rawinsonde measurements at Singapore. The zonal winds at Singapore are a standard reference for QBO variability (Naujokat 1986; Tung and Yang 1994a), and these comparisons demonstrate that the UKMO analyses depict the QBO in a reasonable manner (although with some-

Corresponding author address: Dr. William J. Randel, Atmospheric Chemistry Division, National Center for Atmospheric Research, P.O. Box 3000, Boulder, CO 80307-3000.
E-mail: randel@ucar.edu

what diminished intensity). Second, we examine the space–time structure of QBO circulation anomalies over the globe based on the UKMO data. An intriguing aspect of the QBO is the link to extratropics that is apparent in stratospheric winds and temperatures (Tucker and Hopwood 1968; Dunkerton and Baldwin 1992; Randel and Cobb 1994) and trace constituent data, particularly ozone (e.g., Bowman 1989; Tung and Yang 1994a; Hollandsworth et al. 1995; Randel and Wu 1996). One aim here is to derive and isolate the QBO component of the mean vertical circulation, in both Tropics and extratropics. To this end we calculate components of the residual mean meridional circulation from the coupled thermodynamic and mass continuity equations, utilizing radiative heating rates derived from UKMO temperatures and contemporaneous ozone and water vapor data. The results show coherent QBO variations in both Tropics and extratropics, spanning much of the globe. A longer time record of satellite radiance measurements (spanning 1979–1994) reveals similar QBO patterns in global stratospheric temperatures, suggesting that results from the relatively short UKMO record are robust.

2. Data and analyses

a. UKMO data and residual circulation

The UKMO stratospheric analyses used here are output of a data assimilation system (Swinbank and O'Neill 1994a). This system uses a global numerical model of the atmosphere, with fields continuously adjusted toward available wind and temperature observations as the model is integrated forward in time. Output of these analyses include temperatures and three-dimensional winds, spanning pressure levels of 1000–0.32 mb (0–57 km). The focus here is on stratospheric levels of 100–0.68 mb (we omit data from the upper two levels, as these are near the lid of the numerical model). We use the temperature and horizontal wind analyses and derive vertical velocities from thermodynamic balance as discussed below. The time period analyzed here covers November 1991–October 1998.

Estimates of the residual mean meridional circulation components $\overline{v^*}$ and $\overline{w^*}$ are derived from the coupled thermodynamic and continuity equations (Andrews et al. 1987; Rosenlof 1995; Eluszkiewicz et al. 1996)

$$\frac{\partial \overline{T}}{\partial t} + \overline{v^*}\,\overline{T}_y + \overline{w^*}\frac{H}{R}N^2 = \overline{Q} \qquad (1)$$

and

$$\frac{1}{a\cos\phi}\frac{\partial}{\partial\phi}(\cos\phi\,\overline{v^*}) + \frac{1}{\rho_o}\frac{\partial}{\partial z}(\rho_o\overline{w^*}) = 0. \qquad (2)$$

Here notation follows Andrews et al. (1987). We have neglected an eddy covariance term in Eq. (1), as direct calculations show that it is relatively small, particularly for monthly timescale variations (Gille et al. 1987; Eluszkiewicz et al. 1996). We use an accurate radiative heating code (Olaguer et al. 1992) to estimate $\overline{Q}$, based on input of UKMO temperatures and time-varying ozone, methane and water vapor fields from the Halogen Occultation Experiment (HALOE) (Russell et al. 1993). Other radiative trace gases are kept at climatological (constant) values. Equations (1)–(2) are solved iteratively to obtain values for $\overline{v^*}$ and $\overline{w^*}$. This choice of calculating $\overline{w^*}$ via thermodynamic balance follows the results of Weaver et al. (1993). They compare this technique with $\overline{w^*}$ derived from assimilated data alone (from the NASA/Goddard assimilation), and show more realistic behavior using the radiative–thermodynamic estimate.

b. Satellite radiance data

We also include longer time series of stratospheric temperature measurements (spanning 1979–1994) to illustrate the robust character of the QBO structures derived from the relatively short UKMO record. These data are derived from stratospheric radiance measurements taken by the Stratospheric Sounding Unit (SSU) on board a series of NOAA operational satellite platforms. The long time series presented here are a new product that have been adjusted using temporal overlap between satellites to provide homogeneous time series of stratospheric radiance measurements. The specific radiance data used here are derived from differences between nadir and off-nadir SSU measurements, yielding so-called synthetic channel radiances (see Nash 1988). The synthetic channels chosen to highlight QBO variations here are termed 15*X* and 35*X*; the weighting functions for these channels peak near 50 mb (21 km) and 5 mb (38 km), respectively, with a thickness of ~10 km (these weighting functions are shown in Fig. 19).

c. Isolation of the QBO

The analyses here are based on monthly averaged data. Interannual anomalies are calculated as deviations from the mean annual cycle during 1993–97 (1992 is omitted because of anomalous warming associated with the Mt. Pinatubo volcanic eruption in 1991). Variations in all fields associated with the QBO are isolated by fitting the full interannual anomalies with a linear regression of the form

$$U_{\mathrm{QBO}}(t) = \alpha \cdot \mathrm{EOF1}(t) + \beta \cdot \mathrm{EOF2}(t). \qquad (3)$$

Here EOF1 and EOF2 are temporally orthogonal QBO reference time series, derived from optimal linear combinations of the zonal winds over 70–10 mb [shown in Fig. 3 of Wallace et al. (1993)]: these two time series explain more than 90% of the QBO zonal wind variance during 1956–1990 (Wallace et al. 1993). In order to include seasonality, we choose $\alpha = A_1 + A_2 \sin\omega t + A_3 \cos\omega t$ with $\omega = 2\pi/(365\ \mathrm{days})$; the coefficients A_1–A_3 (and likewise B_1–B_3 for β) are determined by least squares regression. Overall, Eq. (3) acts as an accurate

digital filter to isolate time variations that are coherent with the zonal wind QBO [see further details in Randel and Wu (1996)].

3. Comparisons with Singapore rawinsonde data

Rawinsonde observations from Singapore (1°N, 104°E) are often used as a standard reference for the QBO winds (e.g., Naujokat 1986). Figure 1 shows comparisons at 50, 30, and 10 mb between zonal winds measured at Singapore, zonal winds from UKMO analyses interpolated to the location of Singapore, and equatorial zonal-mean zonal winds from UKMO. The Singapore measurements have been deseasonalized identically to the UKMO data (using the 1993–97 mean). The overall QBO variations are similar between the UKMO and Singapore data and the agreement is reasonably good at 50 mb. However, these comparisons show systematic biases in the strength of the maximum winds in the upper levels, with largest biases at 10 mb. For the data at 30 and 10 mb, the UKMO values at Singapore come closer to the rawinsonde data than the zonal means, but biases are still evident. Climatological studies based on a limited number of equatorial radiosonde stations (e.g., Dunkerton and Delisi 1985) have suggested that there is little zonal structure to the QBO in the lower stratosphere, so that the longitudinal variations implied in the UKMO data in Fig. 1 (i.e., differences between zonal means and Singapore location winds) are possibly an artifact of the assimilation process. However, recent analysis of satellite wind measurements (Ortland et al. 1996) suggests some significant zonal asymmetries may be associated with the westerly phase of the QBO in the middle stratosphere (D. Ortland 1996, personal communication), and a similar result is obtained in a recent three-dimensional model simulation (Hamilton 1998). These asymmetries are related to the cross-equatorial propagation of stationary planetary waves from the winter hemisphere during QBO westerlies. However, such zonal structure is not likely to be a large effect here, as the UKMO–radiosonde biases in Fig. 1 are similar for both easterly and westerly phases.

Assimilation experiments confirm that radiosonde wind observations are important for the representation of the QBO in the UKMO wind analyses. At lower levels there are significantly more data, which leads to the good agreement between UKMO and Singapore at 50 mb. At higher levels, where there are less radiosondes, the UKMO wind analyses are more dependent on satellite temperature soundings. Singapore is one of the most reliable radiosonde stations in the Tropics; although the Singapore observations are regularly input into the UKMO analyses, supporting data from other stations are rather sparse. This lack of wind observations is consistent with the poorer agreement with Singapore winds at 10 and 30 mb, compared to 50 mb.

Figure 2 shows similar comparisons between Sin-

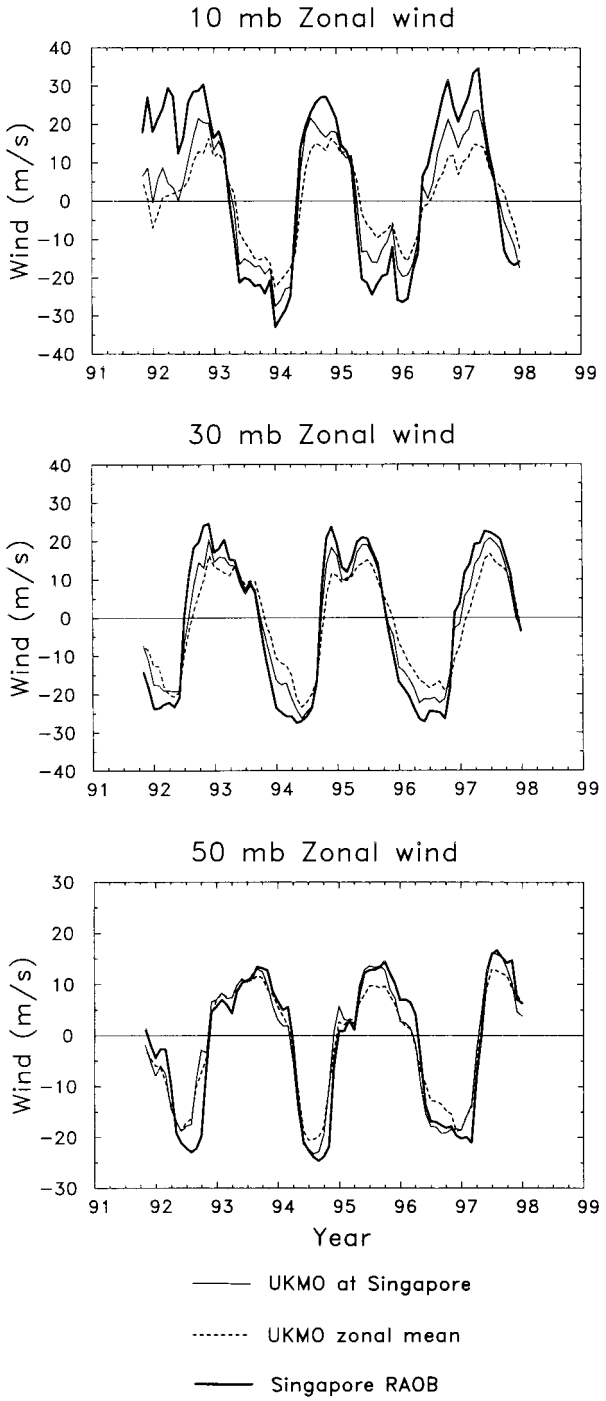

FIG. 1. Time series of monthly mean zonal wind anomalies derived from rawinsonde measurements at Singapore, UKMO analyses interpolated to Singapore, and UKMO zonal-mean equatorial winds. Results are shown at 10 mb (top), 30 mb (middle), and 50 mb (bottom).

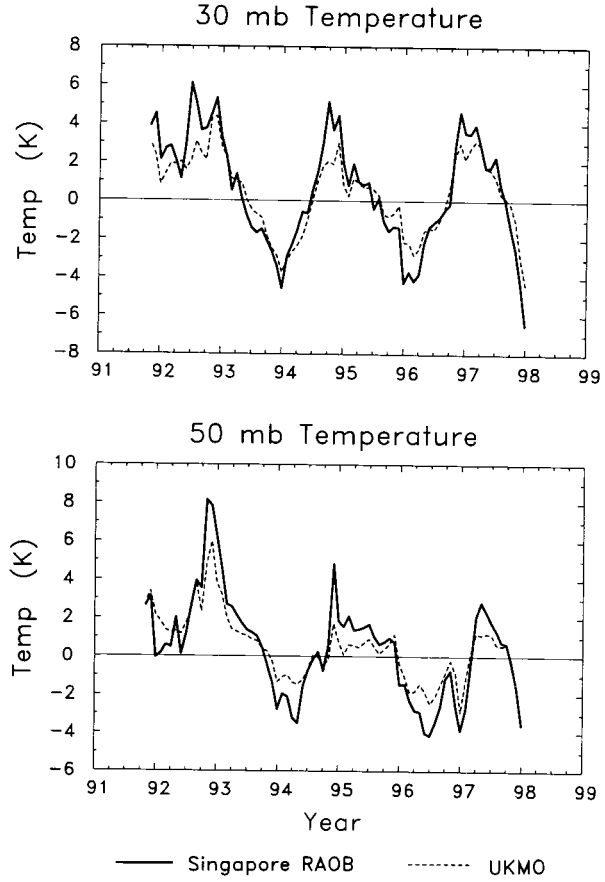

FIG. 2. Time series of monthly mean temperature anomalies from Singapore rawinsonde data and UKMO equatorial zonal-mean analyses, at 30 mb (top) and 50 mb (bottom).

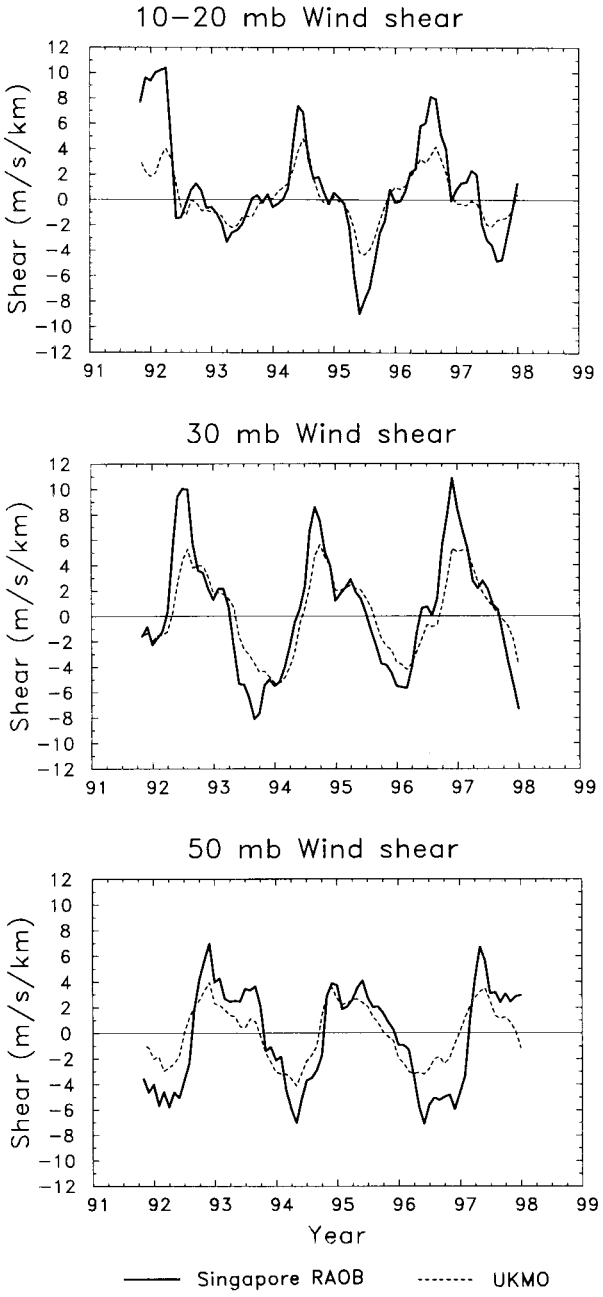

FIG. 3. Time series of anomalies in zonal wind vertical shear, derived from Singapore rawinsonde data and UKMO zonal-mean equatorial analyses, for 10–20 mb (top), 30 mb (middle), and 50 mb (bottom).

gapore rawinsonde temperatures and zonal-mean UKMO temperatures at 50 and 30 mb. These time series show clear QBO variations in both datasets, but indicate a systematic underestimate of extrema in the UKMO analyses: the rms temperature variations from UKMO zonal means is only 65%–70% that of the radiosondes. Figure 3 compares time series of the vertical shear of the zonal wind ($\overline{u}_z$), which is an important dynamical quantity for two reasons. First, it is related to the temperature perturbations via thermal wind balance [following the notation of Andrews et al. (1987), Eq. (8.2.1)]:

$$\overline{u}_z = -\left(\frac{R}{H\beta}\right)\overline{T}_{yy}, \tag{4a}$$

where for QBO variations centered on the equator with meridional scale L

$$\overline{u}_z \approx \left(\frac{R}{H\beta}\right)\frac{\delta\overline{T}}{L^2}. \tag{4b}$$

Secondly, $\overline{u}_z$ is proportional to the mean vertical velocity (as shown below). Comparisons are shown in Fig. 3 for $\overline{u}_z$ at 50 and 30 mb (using centered differences), and for the 10–20 mb shear (because 10 mb is the upper level of available rawinsonde data). These comparisons show reasonable temporal agreement between the zonal-mean UKMO analyses and Singapore data, but indicate that the UKMO analyses underestimate the maximum

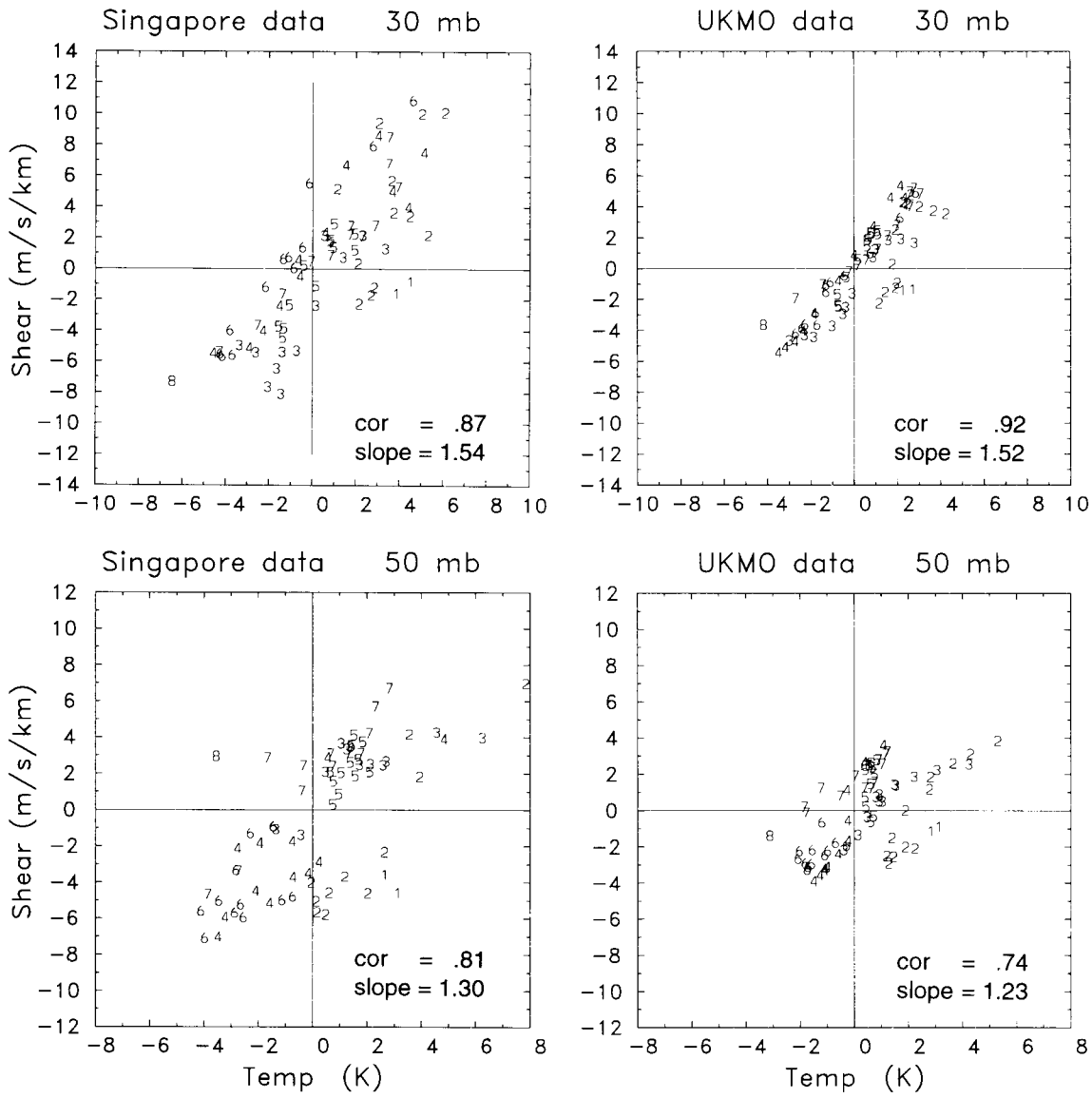

FIG. 4. Scatterplots of vertical shear of zonal wind vs temperature anomalies, for Singapore rawinsonde data (left panels) and UKMO equatorial zonal means (right), at 30 mb (top) and 50 mb (bottom). The numbers on the scatterplots refer to the year of the data (2 = 1992, etc.). Correlations and slopes are calculated using data over 1993–97 [slope units are (m s^{-1}/km) per (K)].

values, particularly for the strong westerly shears at upper levels. The ratio of rms amplitudes between the UKMO zonal means and radiosonde data is 0.56, 0.65, and 0.47 for the 50 mb, 30 mb, and 10–20 mb data in Fig. 3, respectively.

Because of limitations in the vertical resolution of the UKMO analyses, they are not able to capture the sharpness of the wind shear ($\overline{u}_z$), particularly the strong wind shear that occurs at the onset of the westerlies. At higher altitudes, the UKMO analyses are largely produced from satellite temperature soundings, which have poor vertical resolution, so one would expect the ability of the UKMO data to represent the QBO shear zones to be worse at higher levels.

Figure 4 shows scatterplots of the wind shear ($\overline{u}_z$) versus temperature anomalies ($\delta\overline{T}$) at 50 and 30 mb, for both Singapore rawinsonde measurements and zonal-mean UKMO analyses. These scatterplots test the thermal wind relationship [expressed in Eq. (4)] in both datasets. Overall, strong correlations are seen in both radiosonde and UKMO data, although careful inspection shows that data during 1991–92 at both altitudes falls somewhat to the right of the rest of the distributions (particularly at 50 mb). This is likely due to anomalously warm tropical temperatures associated with the eruption of Mt. Pinatubo in June 1991 (Labitzke and McCormick 1992; Angell 1993). These Pinatubo temperature anomalies exhibit a broader meridional scale than the QBO

(see Fig. 10 below), and thus have less impact on ($\overline{u}_z$) [via Eq. (4b)]. Calculation of the derived slopes ($\delta\overline{u}_z/\delta\overline{T}$), using only data over 1993–97, gives values consistent with a meridional scale $L \approx$ 1000–1200 km in Eq. (4).

4. Global QBO anomalies

a. Zonal wind and temperature

The remainder of the analyses here focus on the zonal-mean UKMO anomalies, in particular the components that are coherent with the QBO [e.g., isolated using Eq. (3)]. Figure 5 shows altitude–time sections of the monthly mean zonal winds over the equator for the full interannual anomalies (smoothed slightly in time using a 1–1–1 running mean), the QBO component, and the residual. The QBO component captures practically all of the interannual variance below 10 mb; these anomalies show largest amplitudes over 20–35 km, with maxima near 25–30 km. A continuous QBO signal can be traced as high as the stratopause (~45–50 km), where the winds are approximately out of phase with those near 30 km, but here the magnitude of the QBO component is of the same size as the residual. Baldwin and Dunkerton (1991) note a similar upper-stratospheric reversal in QBO winds derived from National Centers for Environmental Prediction (NCEP) stratospheric analyses.

Latitude–time evolution of the full and QBO-fit zonal wind anomalies at 32 mb (24 km) is shown in Fig. 6. The tropical QBO anomalies are centered over the equator, with a meridional extent spanning ~20°N–S. There is also some projection of the high-latitude zonal wind anomalies in each hemisphere onto the QBO during this short 7-yr sample. These are phased such that a stronger polar vortex is associated with tropical QBO westerlies [as documented in longer time series by Holton and Tan (1980), (1982) and Dunkerton and Baldwin (1992) and found in the modeling results of O'Sullivan and Young (1992), O'Sullivan and Dunkerton (1994), and Hamilton (1998)].

Figure 7 summarizes the QBO zonal wind structure derived from these data. This shows the equivalent harmonic amplitude of the QBO-fit anomalies, calculated as the anomaly rms value during 1991–97 times $\sqrt{2}$ (this is the equivalent amplitude of a harmonic oscillation). Figure 8 shows a comparison of the UKMO QBO zonal wind amplitude near 30 mb with the structure derived by Dunkerton and Delisi (1985) from a long record of rawinsonde data. This shows that the UKMO data underestimate the QBO amplitude by ~30% at 30 mb (similar to the results seen in Fig. 1), but that the latitudinal structures are similar. Figure 7 also shows weak amplitude maxima in the midlatitude upper stratosphere and over high latitudes of both hemispheres; the structure and timing of these extratropical anomalies are shown in Fig. 6 and further below.

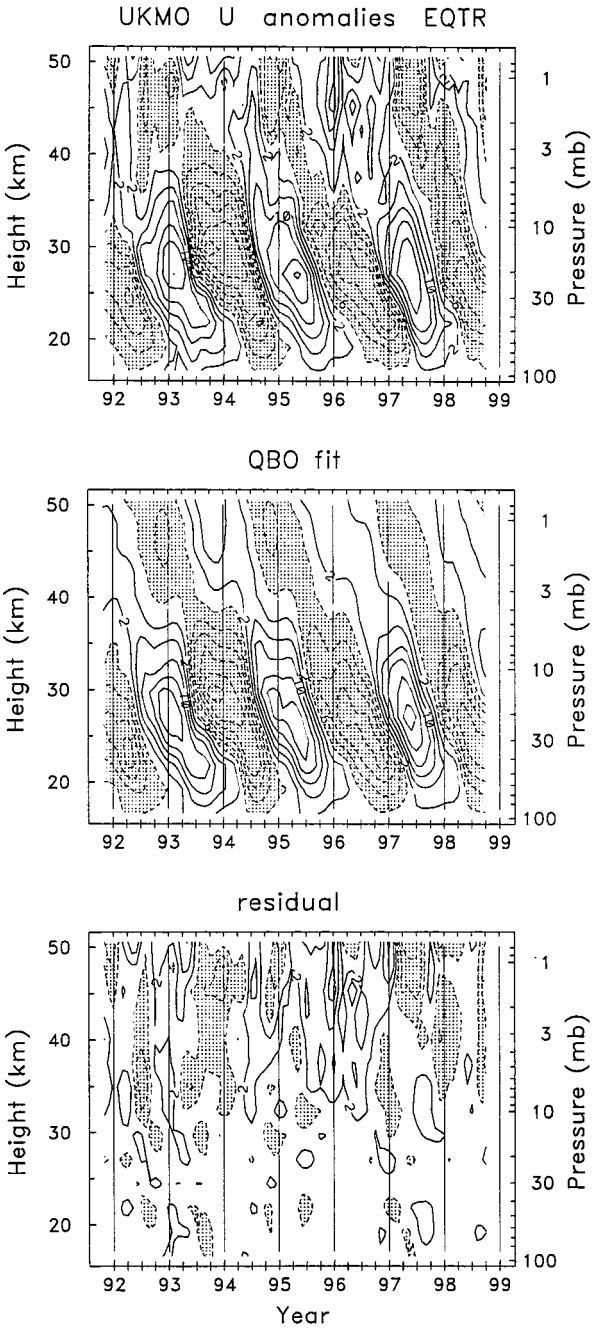

FIG. 5. Altitude–time sections of UKMO zonal-mean zonal wind anomalies at the equator. Shown are the full anomalies (top), the QBO statistical fit (middle), and the residual (bottom). Contours are ±2, 6, 10, · · · m s^{-1}.

Zonal-mean temperature anomalies at the equator are shown in Fig. 9, including the full anomalies, the QBO fit, and the residuals. A clear QBO signal is observed in the full anomaly field, with downward propagation apparent over a deep altitude range (~20–45 km). The QBO filtered temperature anomalies exhibit maxima in

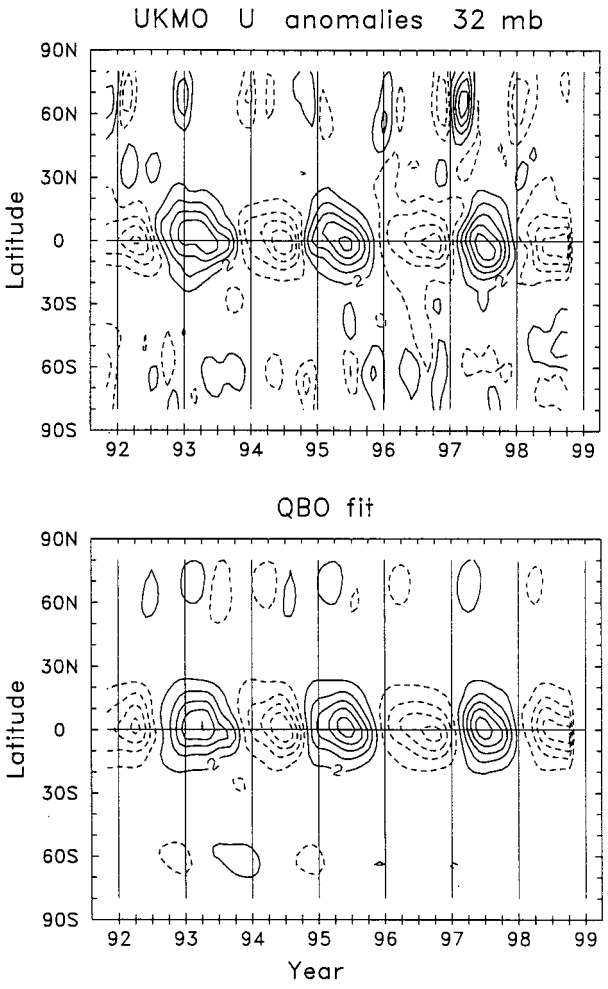

FIG. 6. Latitude–time sections of UKMO zonal wind anomalies at 32 mb. Top panel shows the full anomalies, and bottom panel is the statistical QBO fit. Contours are ±2, 6, 10, · · · m s^{-1}.

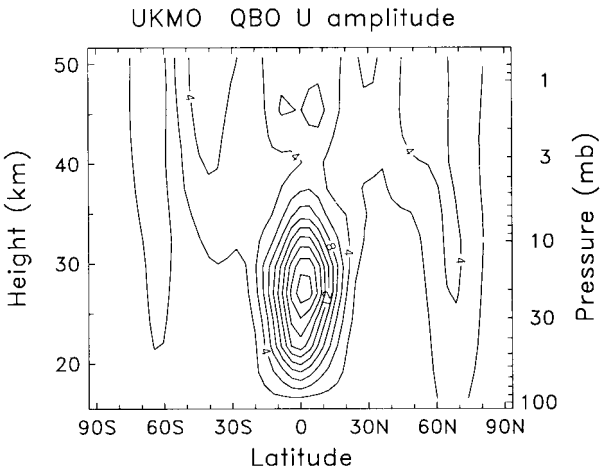

FIG. 7. Meridional cross section of the equivalent harmonic amplitude of the QBO zonal wind anomalies from UKMO data (calculated as described in text). Units are meters per second.

the lower stratosphere (~25–27 km) that move downward in time, plus somewhat weaker upper stratospheric signals with less vertical tilt; the lower and upper stratosphere maxima are approximately out of phase. Note that these temperatures are in thermal wind balance with the QBO zonal wind shear $\overline{u}_z$ (see Fig. 4), and the two temperature maxima coincide with strong shear zones above and below the maximum QBO winds. The temperature residuals in Fig. 9 show a large positive anomaly (>3 K) in the lower stratosphere during 1991–93 due to Mt. Pinatubo. There are also relatively large temperature residuals above 30 km (as large as the QBO signal). The large positive residual near 50 km at the beginning of the record is an artifact related to problems with the UKMO data assimilation system; these were resolved by changing the observation quality control and some other aspects of the assimilation [for further details see Swinbank and O'Neill (1994a)].

Figure 10 shows the latitude-time evolution of temperature anomalies at 32 mb (~24 km). The QBO component shows maxima centered over the equator with narrow meridional extent (~10°–15°N–S). Furthermore, there are smaller amplitude QBO patterns observed in low-middle latitudes (~20°–40°) of both hemispheres, approximately out of phase with the equatorial variations (somewhat larger in the NH); note these patterns are evident in the full anomaly field, and are not a result of the QBO filtering. There are also projections of the QBO over polar regions, but this signal is not large compared to the residual. The spatial structure of the residual is quite distinct from the QBO patterns, showing broad latitudinal maxima over 30°N–S for the 1991–93 warm Pinatubo anomaly. Note that, because the thermal wind relationship [Eq. (2a)] depends on the temperature meridional curvature $\overline{T}_{yy}$, the zonal wind shear anomalies associated with these broadscale residuals are much smaller than the QBO signal. Thus the largest

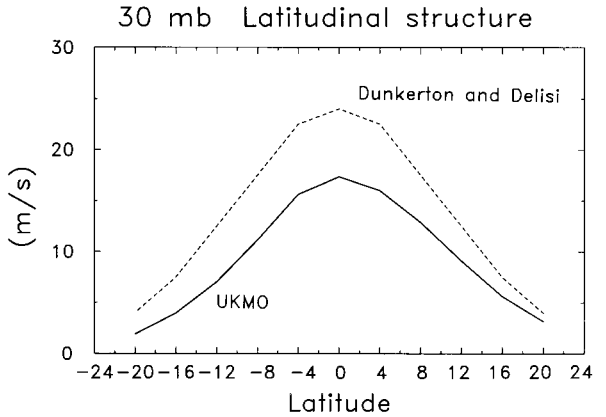

FIG. 8. Latitudinal profile of the QBO zonal wind equivalent harmonic amplitude near 30 mb derived from UKMO data, and that derived from long records of rawinsonde measurements by Dunkerton and Delisi (1985).

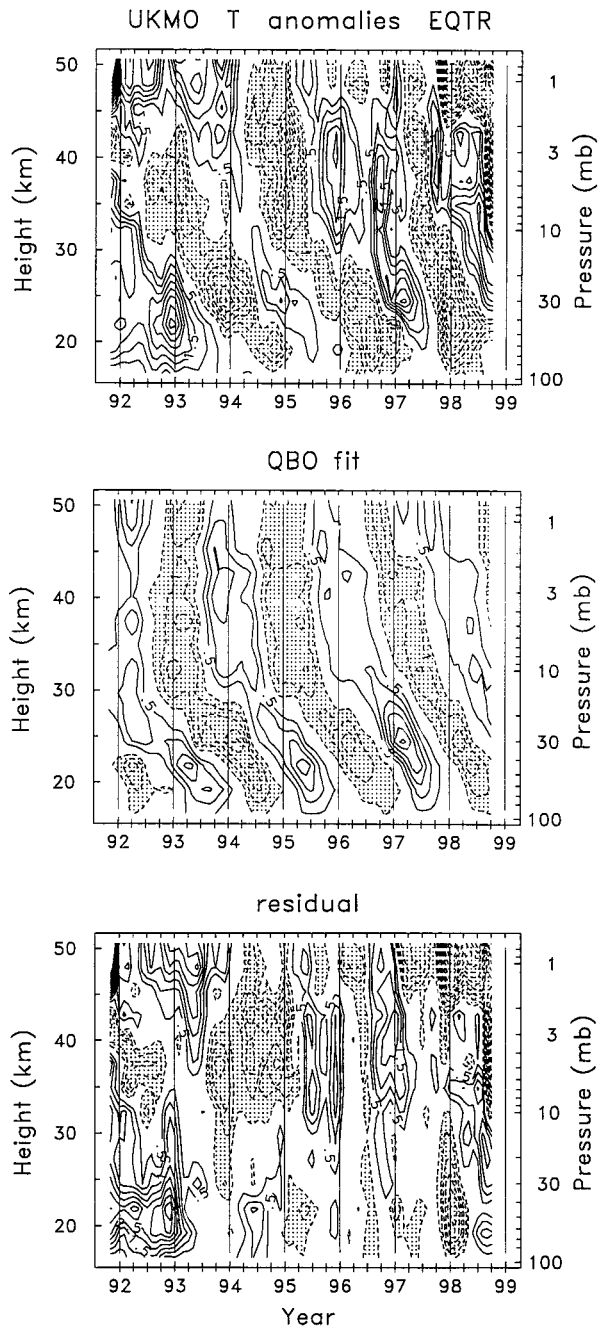

FIG. 9. Altitude-time sections of UKMO zonal-mean equatorial temperature anomalies. Shown are the full anomalies (top), the QBO statistical fit (middle), and the residual (bottom). Contours are ±0.5, 1.0, 1.5, · · · K.

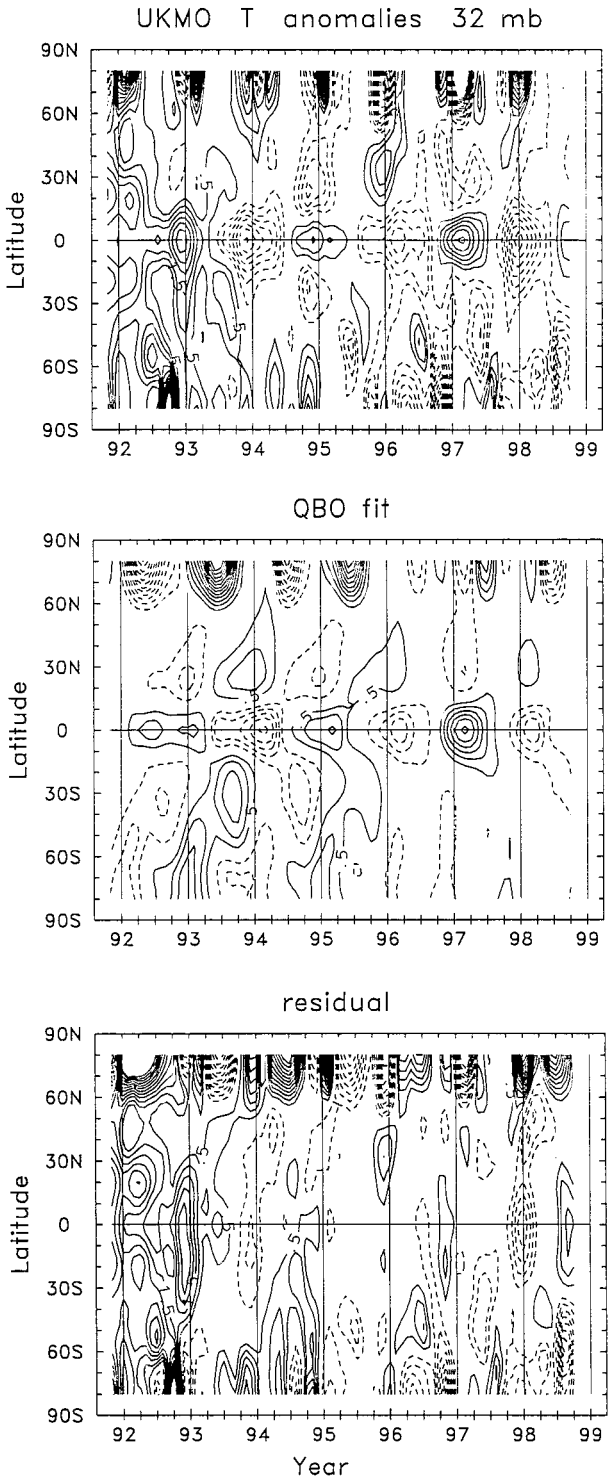

FIG. 10. Latitude-time sections of UKMO temperature anomalies at 32 mb. Shown are the full anomalies (top), the QBO statistical fit (middle), and the residual (bottom). Contours are ±0.5, 1.0, 1.5, · · · K.

temperature residuals in 1991–92 are balanced with relatively small wind shear anomalies, which accounts for the ''outlier'' nature of these data points in Fig. 4.

The latitudinal structure of the full and QBO fit temperature anomalies at 3.2 mb (~40 km) is shown in Fig. 11. There is an equatorially centered QBO component, approximately out of phase with temperatures at 32 mb

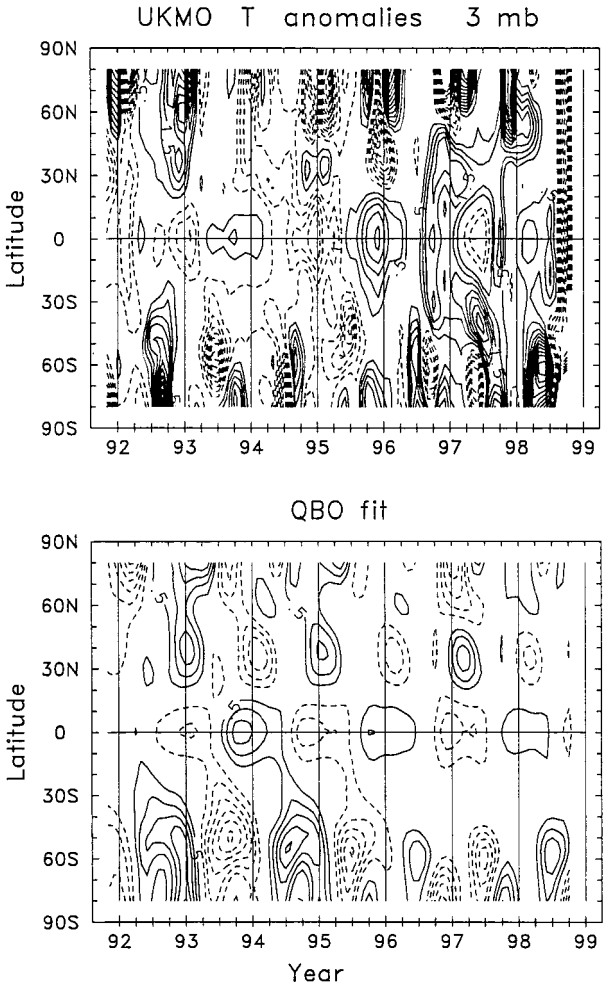

FIG. 11. Full and QBO-fit UKMO temperature anomalies at 3 mb. Contours are ± 0.5, 1.0, 1.5, $\cdots$ K.

(Fig. 10). In addition, there are QBO temperature maxima in middle latitudes of both hemispheres, and we note again that these are evident in the full anomaly field. An important aspect of these midlatitude maxima is that they occur primarily during winter of the respective hemispheres (i.e., they are seasonally synchronized).

b. Heating rates and residual circulations

Figure 12 shows the interannual anomalies in zonal-mean radiative heating rates ($\overline{Q}$) over the equator, calculated using the observed temperature and constituent data as discussed in section 2. We note that our calculations do not include the radiative effects of Pinatubo aerosols; these contribute substantial positive anomalies in the lower stratosphere during 1991–92 (Eluszkiewicz et al. 1997), but do not strongly influence the QBO results of focus here. Clear downward propagating QBO patterns are observed in the (unfiltered) data in Fig. 12. Time-mean background values of ($\overline{Q}$) at the equator are of order 0.2, 0.6, and 1.0 K/day at 32, 10, and 3.2 mb, respectively, so that these interannual anomalies are approximately 10%–20% of background values.

In order to determine the relative contribution of temperature versus constituent variations in the heating rates, a separate calculation was performed wherein the constituents were held constant (i.e., only temperature variations contributed to the heating rates). This result is also shown in Fig. 12, along with the difference between the full and constant constituent calculations (i.e., the component due primarily to constituent variations). These latter heating anomalies are primarily due to ozone variations (associated with the QBO); note the similar space–time patterns observed in the HALOE ozone anomalies shown in Fig. 12 [these exhibit a dominant QBO component, similar to SAGE II data results in Zawodny and McCormick (1991) and Randel and Wu (1996)]. The comparisons in Fig. 12 show that both temperature and constituents (mainly ozone) contribute substantial fractions to the total interannual heating anomalies. An important detail here is that the temperature and ozone contributions to the heating rate are in phase in the upper stratosphere (where the ozone and temperature anomalies are oppositely signed), whereas their effects on the radiative heating tend to cancel in the lower stratosphere (where ozone and temperature are in phase—compare the ozone anomalies in Fig. 12 with the temperatures in Fig. 9). Thus the radiative contribution of ozone acts to reduce the $\overline{Q}$ anomalies in the lower stratosphere (compared to the effects of temperature alone), and this results in less intense interannual variations in $\overline{Q}$ below 30 km (and likewise for $\overline{w^*}$ derived from thermodynamic balance).

Figure 13 shows altitude–time sections of derived residual mean vertical velocity ($\overline{w^*}$) anomalies for both full and QBO-fit components. Note the similarity of $\overline{w^*}$ (Fig. 13) to $\overline{Q}$ (Fig. 12), due to the near thermodynamic balance

$$\overline{w^*}\frac{H}{R}N^2 \approx \overline{Q}$$

{the remaining terms in the thermodynamic budget [Eq. (1)] are small, in particular $\partial\overline{T}/\partial t$}. Largest absolute variations in $\overline{w^*}$ are observed in the upper stratosphere over $\sim$35–45 km. The anomalies are of order ± 0.1 km/month in the lower stratosphere, and ± 0.5 km/month in the upper stratosphere (or 0.04–0.20 mm s^{-1}); these values are about twice as large as the QBO $\overline{w^*}$ anomalies derived by Hasebe (1994), which may be due to an underestimate of QBO temperature anomalies in that work. Figure 14 shows the ''full'' calculated time series of equatorial $\overline{w^*}$ at 32 and 3.2 mb, together with the deseasonalized anomalies and the QBO fits at each pressure level. There is a strong annual cycle in $\overline{w^*}$ at the equator, with a maximum during NH winter and a factor

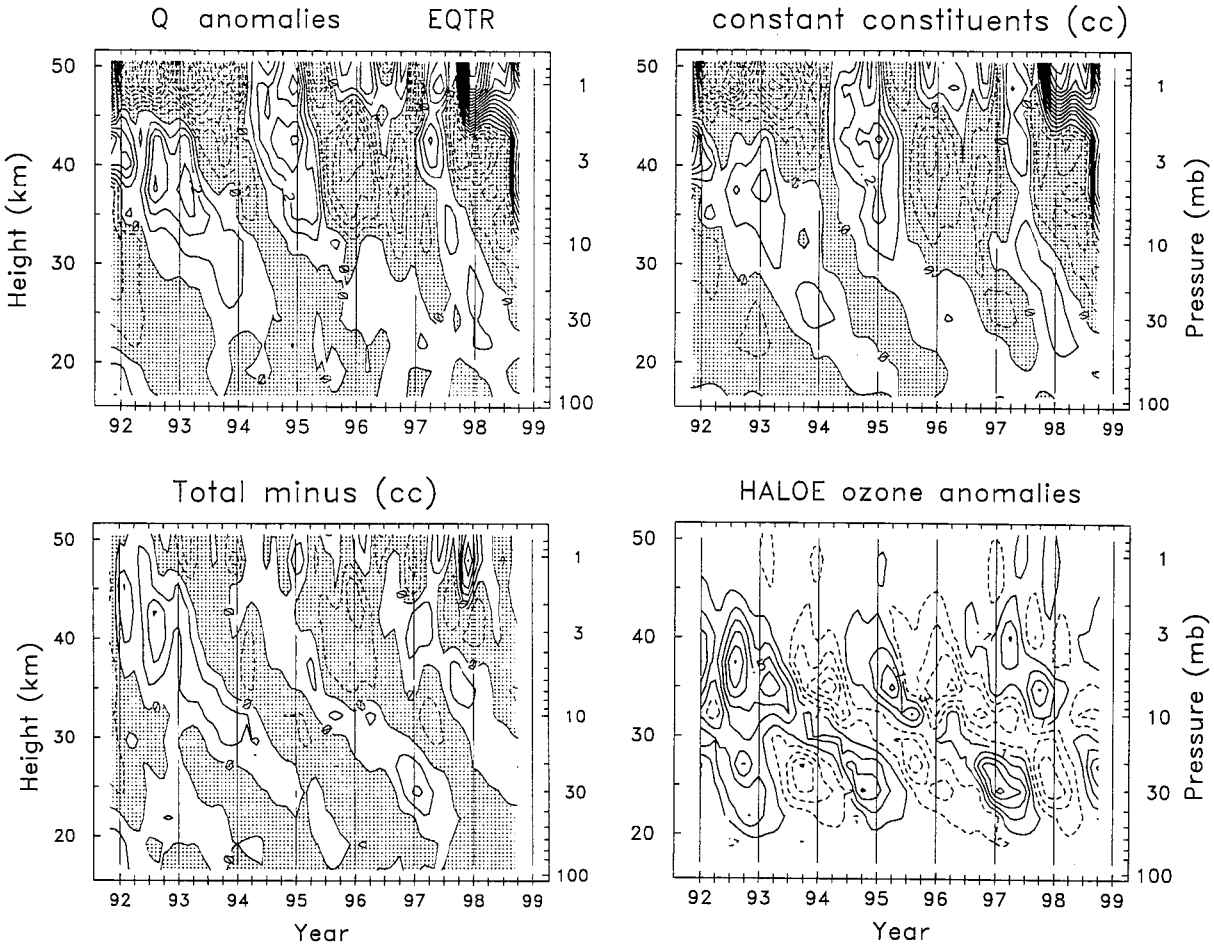

FIG. 12. (upper left) Altitude–time section of equatorial radiative heating anomalies, derived from UKMO temperatures and HALOE constituent fields (as described in text). The important effect of Pinatubo aerosol heating has not been included, and thus details of the 1991–92 results are suspect. Contour interval is 0.1 K/day. (upper right) Results using time-varying temperatures but constant ozone and other constituent concentrations. (lower left) The difference between the upper two panels (i.e., the component associated with constituent changes). (lower right) HALOE interannual ozone anomalies, with contours of ± 0.1, 0.3, 0.5 $\cdots$ ppmv.

of approximately 2(3) seasonal variation at 32 (3.2) mb. The QBO component of $\overline{w^*}$ in Figs. 13–14 captures a large fraction of the interannual variance, but these variations are substantially smaller than the seasonal cycle.

Because the UKMO temperature anomalies are likely underestimates of the actual QBO temperatures (by at least 40% based on Fig. 2), the derived radiative heating ($\overline{Q}$) and vertical velocity ($\overline{w^*}$) estimates are also likely to be too small. For comparison, the calculations were redone with temperature anomalies multiplied by 1.4, and these are included in Fig. 14. These larger temperature anomalies produce relative small change at 3.2 mb, but increase the QBO $\overline{w^*}$ amplitude by approximately 50% at 32 mb. There is a relatively larger effect in the lower stratosphere because of the opposing sign of the ozone radiative heating (discussed above). These larger $\overline{w^*}$ values are probably more realistic estimates of actual QBO variations.

An empirical result derived from these data is that there is a strong linear relationship between QBO anomalies in derived $\overline{w^*}$ and those in $\overline{u}_z$. This is shown in Fig. 15 for data at 32 mb (24 km) and 3.2 mb (40 km). In these results we have used the estimates of $\overline{w^*}$ based on the temperature anomalies increased by a factor of 1.4, and likewise multiplied the observed $\overline{u}_z$ by this same factor [based on Eq. (4b)]. This correlation is due to both $\overline{w^*}$ and $\overline{u}_z$ being related to temperature ($\overline{T}$): $\overline{w^*}$ is proportional to $\overline{Q}$, which is a strong function of $\overline{T}$ (Figs. 9–12), and $\overline{u}_z$ is proportional to $\overline{T}$ via thermal wind balance [Eq. (4b) and Fig. 4]. The slope of the relationship ($\delta\overline{w^*}/\delta\overline{u}_z$) changes by an order of magnitude between the lower and upper stratosphere, as shown in Fig. 16 (this figure includes results for both the original data and increased temperature anomaly cases). If $\overline{Q}$ is approximated by a Newtonian cooling expression $\overline{Q} = -\alpha\overline{T}$, then the approximate thermodynamic balance

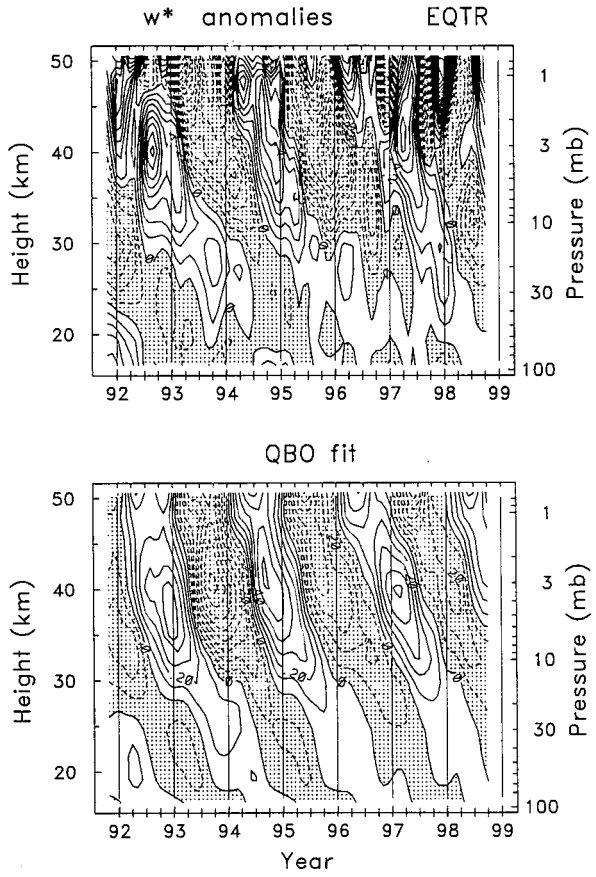

FIG. 13. Altitude–time sections of interannual anomalies in residual mean vertical velocity ($\overline{w^*}$) at the equator, for the full field (top) and QBO-fit components (bottom). Contours interval is 0.1 km/month (multiply by 0.4 to get values in mm s^{-1}).

$$\overline{w^*}\frac{H}{R}N^2 \approx \overline{Q},$$

may be combined with thermal wind [Eq. (4b)] to obtain $(\delta\overline{w^*}/\delta\overline{u}_z) \approx$ const $*\alpha$ (where α is the inverse radiative damping timescale). The observed order of magnitude change in $(\delta\overline{w^*}/\delta\overline{u}_z)$ is consistent with a similar variation in radiative damping times (α^{-1}) between the lower (~50 days) and upper stratosphere (~6 days) (see Gille and Lyjak 1986). These empirical results provide an easy method to estimate equatorial $\overline{w^*}$ anomalies from more readily available estimates of $\overline{u}_z$ (i.e., from the Singapore record).

Latitude–time variations in $\overline{w^*}$ anomalies at 32 and 3.2 mb are shown in Fig. 17 for both the full field and QBO components (using the original UKMO temperature calculations). The QBO component explains a majority of the interannual variance at 3.2 mb; the QBO patterns are clearly seen in the unfiltered data. In contrast, the ''full'' interannual anomalies at 32 mb have substantial non-QBO components; we do not know if this variance is realistic or due to inaccuracies in estimation of $\overline{w^*}$ anomalies in the lower stratosphere.

The $\overline{w^*}$ QBO patterns in Fig. 17 show maxima over the equator at each level, with secondary out-of-phase patterns over NH and SH midlatitudes. Additionally, these anomalies are out of phase vertically between 32 and 3.2 mb. These $\overline{w^*}$ anomalies have similar patterns (with opposite sign) to the temperature anomalies, seen in Figs. 10–11, due to the strong dependence of $\overline{Q}$ on temperature. In the upper stratosphere, midlatitude anomalies are observed over 20°–50°N and 30°–60°S, with similar magnitudes in both hemispheres, whereas in the lower stratosphere the midlatitude response is more coherent in the NH (maxima over 20°–50°N). An important point is that the extratropical maxima in both hemispheres are seasonally synchronized, occurring during midwinter of the respective hemispheres (October–March in the NH and June–September in the SH).

Interannual anomalies in residual mean meridional velocity ($\overline{v^*}$) show substantial non-QBO variance at most altitudes, and these anomalies also exhibit less coherence in the vertical than the $\overline{u}$, $\overline{T}$, or $\overline{w^*}$ anomalies discussed above. Values of $\overline{v^*}$ are derived via continuity from $\overline{w^*}$ [Eq. (2)]. The highly differentiated nature of this calculation warrants caution in interpretation, and we choose not to focus on $\overline{v^*}$ patterns in this study.

Cross sections of QBO anomalies in zonal wind ($\overline{u}$) temperature ($\overline{T}$) and residual mean circulation ($\overline{v^*}$, $\overline{w^*}$) are shown in Fig. 18 for four phases of the QBO cycle during 1993–94. In Fig. 18 vectors representing ($\overline{v^*}$, $\overline{w^*}$) are overlaid on the $\overline{T}$ anomalies. The QBO westerly phase in February 1993 (top panels) is associated with strong wind shears, temperature and vertical velocity anomalies over ~30–40 km, and secondary out-of-phase maxima over 20–25 km. The residual circulation and temperature anomalies exhibit extratropical maxima in the NH (centered near 30°–40°N). Zonal wind anomalies are observed in the upper stratosphere in the Tropics and NH high latitudes. The QBO anomalies during the easterly maximum (February 1994) are approximately mirror images of the westerly phase, in particular there is a much larger midlatitude response in the NH.

The QBO structure during October 1993 shows the descending easterly QBO phase, with strong $\overline{u}_z$, $\overline{T}$, and $\overline{w^*}$ near 25 km. The extratropical temperature anomalies in the lower middle stratosphere (15–30 km) show approximate symmetry between hemispheres. In the upper stratosphere there are much larger temperature and circulation anomalies in the midlatitude SH than in the NH. A very similar but opposite structure is observed in the anomaly fields during the descending westerly phase of the QBO (October 1994). An important aspect of these observations is that the midlatitude component of the QBO is much stronger in the respective winter hemisphere.

5. Comparison with a longer record of satellite data

Figure 19 shows the weighting functions for SSU channels 15*X* and 35*X*. These channels measure the ra-

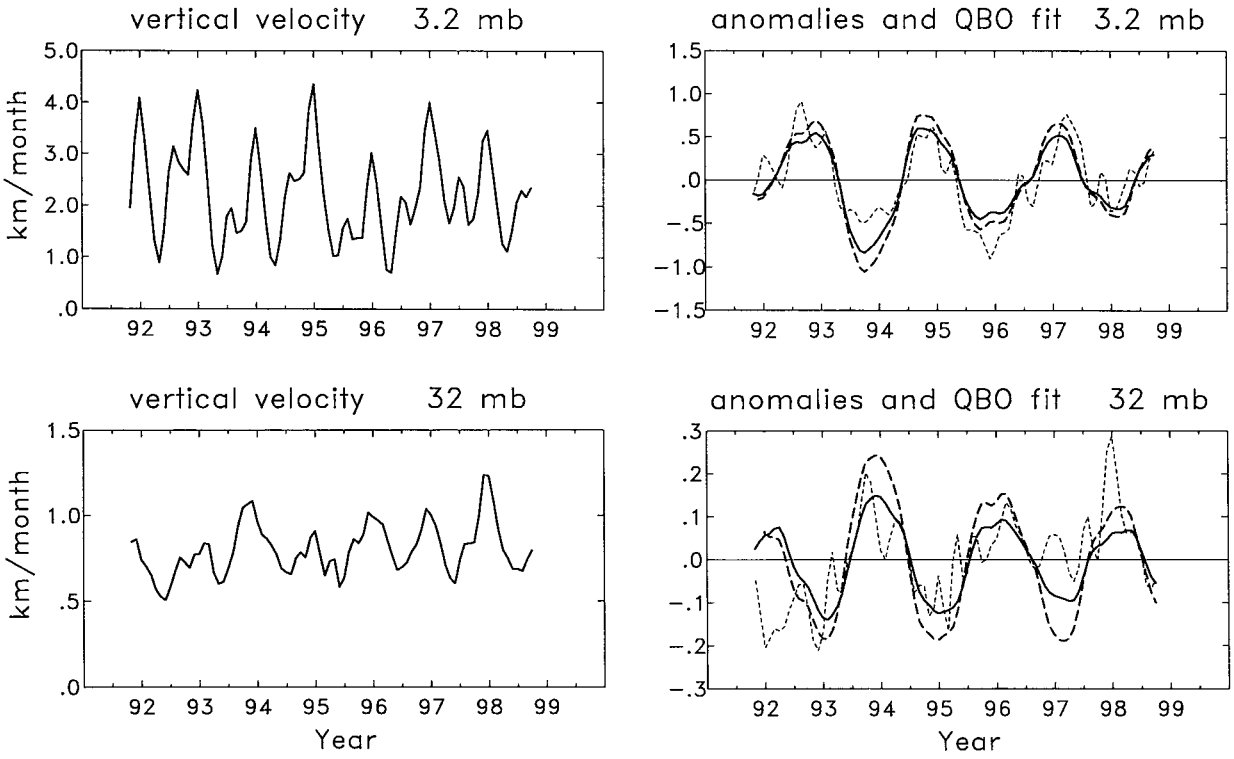

FIG. 14. (left) Time series of $\overline{w^*}$ averaged over 10°N–S at 32 and 3.2 mb, including the respective seasonal cycles. (right) The respective deseasonalized anomalies (light dashed lines), plus the statistical QBO fits (solid lines). Heavy dashed lines denote the QBO fit of $\overline{w^*}$ if temperature anomalies are increased by a factor of 1.4 (as discussed in text). Note the change in scales between the left and right panels.

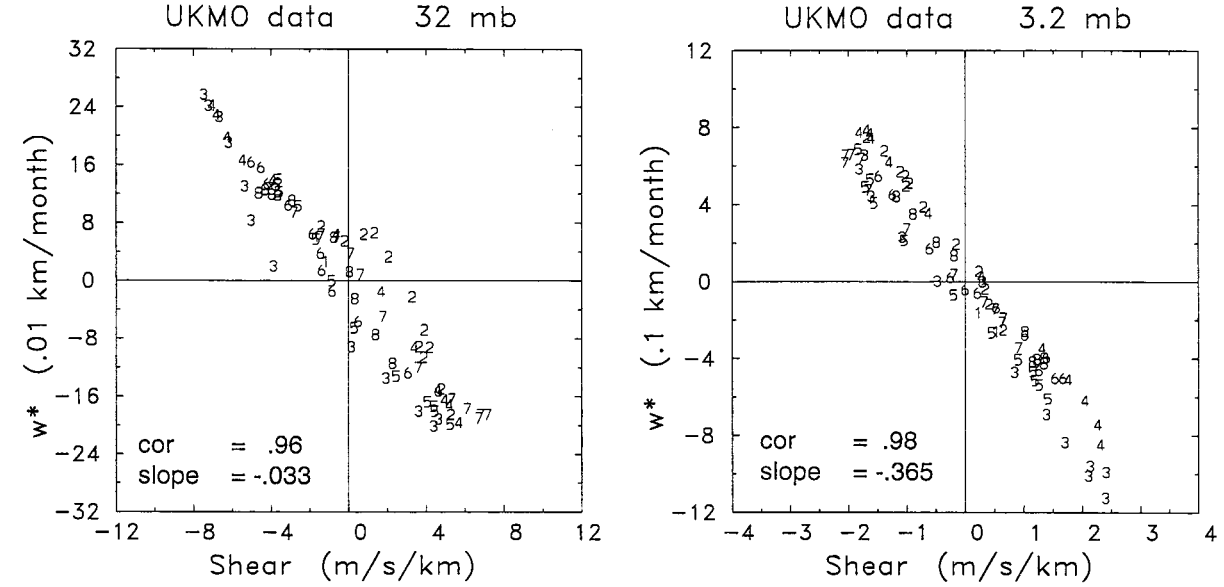

FIG. 15. Scatter diagrams of monthly mean QBO anomalies in residual mean vertical velocity ($\overline{w^*}$) vs vertical shear of the zonal-mean wind ($\overline{u}_z$) over the equator at 32 mb (left) and 3.2 mb (right). Both $\overline{w^*}$ and $\overline{u}_z$ values are based on temperature anomalies multiplied by 1.4 (as discussed in text). The correlation and slope at each position are noted [slope units are (km month^{-1}) per (m s km^{-1})]. Note the factor of 10 scale difference between the $\overline{w^*}$ axes on the two plots.

diance or brightness temperature over layers approximately 10–15 km thick, centered near 22 and 37 km, respectively. Comparison with the temperature anomalies in Fig. 9 shows these layers are near the QBO maxima in the lower and upper stratosphere.

Figure 20 shows latitude–time sections of QBO temperature anomalies derived from SSU 15*X* and 35*X* data spanning 1979–1994. Direct overlap with the UKMO data during November 1991–December 1994 (cf. Figs. 10–11 with Fig. 20) shows reasonable overall agreement in space–time patterns in both Tropics and midlatitudes. The important features of QBO temperature variations seen in the UKMO data are reinforced by the longer record of SSU data. These include: 1) equatorial maxima in the lower and upper stratosphere that are approximately out of phase. Larger amplitude anomalies are found in the lower stratosphere (and these are certainly underestimated by the broad weighting function of SSU 15X). 2) Midlatitude QBO temperature signals in both the lower and upper stratosphere, which are also vertically out of phase. The midlatitude patterns are seasonally synchronized, with maxima during winter of the respective hemispheres. Midlatitude temperature anomalies are larger in the upper stratosphere.

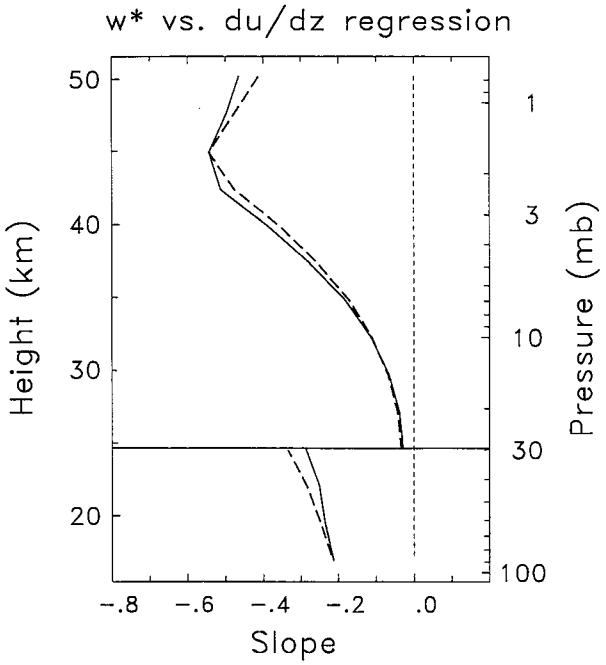

FIG. 16. Slope of the $\overline{w^*}$ versus $\overline{u}_z$ regression vs altitude over the equator. The results are shown multiplied by a factor of 10 below 30 mb for clarity; the slope labels refer to the upper-level curves. The solid lines are for results based on the UKMO temperature and wind anomalies, and the dashed lines for the 40% increased temperature and wind shear calculations. Units are (km/month) per (m s^{-1}/km).

6. Summary and discussion

The 7-yr time series of UKMO stratospheric assimilation data product provides an opportunity to analyze global circulation anomalies associated with the QBO. Comparisons with wind and temperature measurements from Singapore (a standard QBO reference) shows reasonable agreement with UKMO analyses interpolated to Singapore, with a slight underestimate of maximum QBO amplitudes (particularly at 10 mb). Larger biases are observed for UKMO equatorial zonal means, with 20%–40% underestimates for 30–10-mb winds; a similarly sized bias is derived in comparing the UKMO zonal means to the long-term QBO structure derived by Dunkerton and Delisi (1985) (see Fig. 8). Maximum temperature anomalies can be underestimated by 30%–50%, and this corresponds to a similar underestimate of maximum vertical wind shears associated with the QBO. Pawson and Fiorino (1998) report that the QBO wind and temperature amplitudes in the NCEP and ECMWF reanalyses are systematically small also, so this appears to be a consistent problem in current assimilation results. Thermal wind balance in the zonal-mean UKMO data is quantitatively very similar to that derived from Singapore rawinsonde measurements. Apart from the underestimate of maximum values, the space–time patterns of the tropical QBO appear accurately represented in the UKMO assimilated data.

Tropical temperature anomalies associated with the QBO show a maximum near 25 km, together with a secondary maximum in the upper stratosphere near 40 km. These maxima are vertically out of phase, and correspond to oppositely signed vertical shear zones for the QBO zonal winds. QBO temperature anomalies also show substantial midlatitude maxima, peaking near 30°–40° in each hemisphere. The midlatitude maxima also exhibit an out of phase vertical structure between the lower and upper stratosphere, and furthermore exhibit strong seasonal synchronization (with maxima during winter in the respective hemispheres). These midlatitude QBO temperature anomalies are a robust result, as evidenced by their appearance in long-term satellite observations (see Fig. 20). The temperature anomalies are in thermal wind balance with extratropical zonal-mean wind fluctuations, as seen in Fig. 18 and documented in longer time series by Baldwin and Dunkerton (1991) and Baldwin and Tung (1994). Although these extratropical QBO wind anomalies exhibit coherent, repeatable patterns, they do not dominate the interannual variance (the residual interannual variance is larger than the QBO component in extratropics).

Further evidence of the midlatitude effect of the QBO is provided by ozone observations. Long time series of column and profile ozone data show seasonally synchronized QBO maxima centered near 30°–40° N–S (Bowman 1989; Tung and Yang 1994a; Hollandsworth et al. 1995; Randel and Wu 1996). Figure 21 shows global ozone anomalies at 32 mb derived from HALOE data for the time period of interest here (defined as departures from the mean seasonal cycle over 1993–

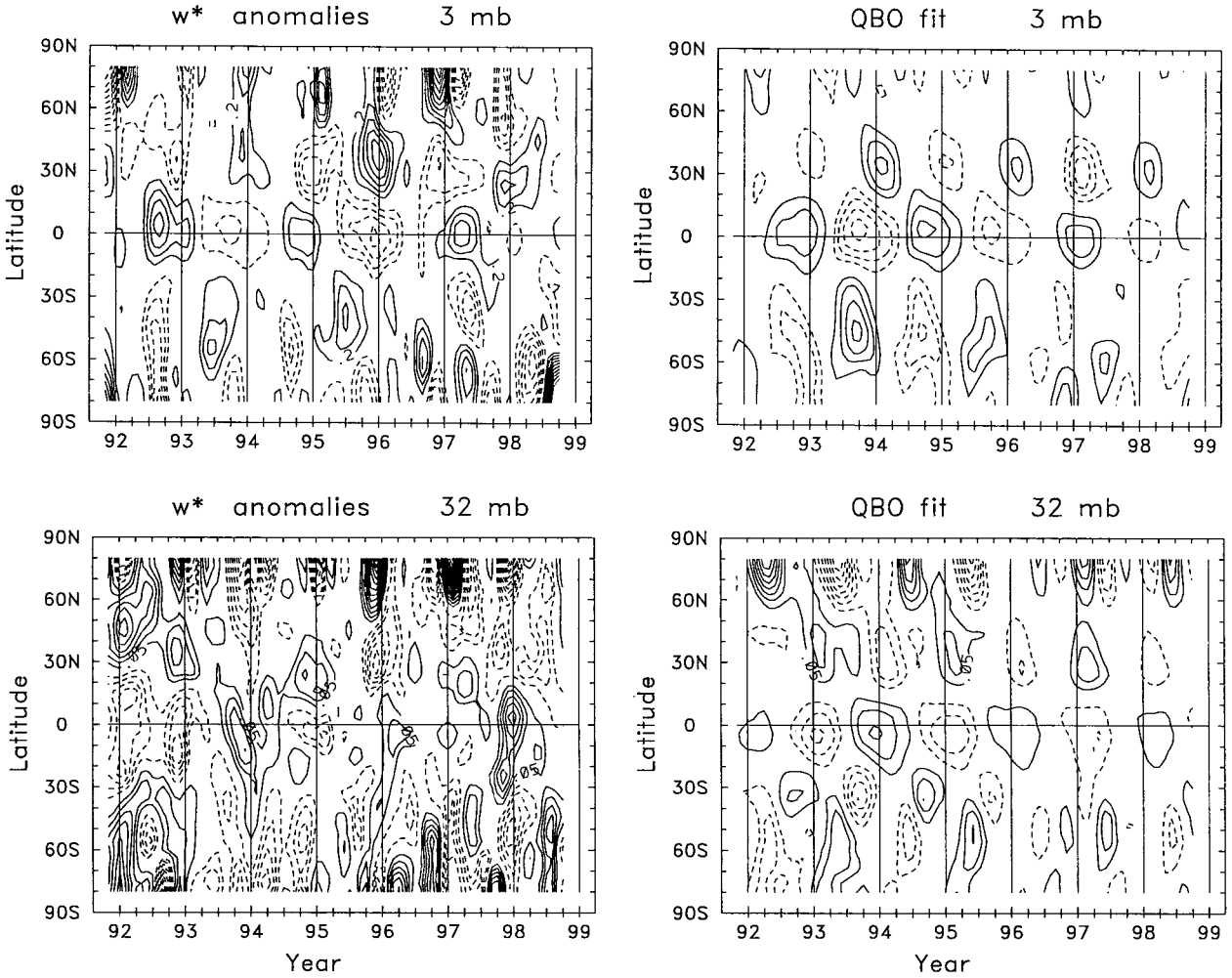

FIG. 17. Latitude–time sections of residual mean vertical velocity ($\overline{w^*}$) interannual anomalies at 3.2 mb (top) and 32 mb (bottom). (Left) the full anomalies and (right) the QBO statistical fit. Contour interval is 2.0 (top) and 0.05 km/month (bottom), with zero contours omitted.

97). These data show pronounced QBO anomalies in Tropics and extratropics, in particular in the NH midlatitudes (no QBO filtering was used in Fig. 21). Both the tropical and midlatitude ozone anomalies are approximately in phase with the QBO temperature patterns shown in Fig. 10, and this is consistent with the results of Randel and Cobb (1994), based on a much longer record. We note that these lower-stratospheric ozone anomalies are approximately out of phase with $\overline{w^*}$ (Fig. 17), although a quadrature relationship is anticipated if ozone transport is dominated by $\overline{w^*}$ advection [see the discussions in Hasebe (1994) and Huang (1996)].

Estimates of QBO anomalies in radiative heating estimates ($\overline{Q}$) and residual mean vertical velocity ($\overline{w^*}$) show coherent downward propagating tropical QBO anomalies. QBO variations in radiative heating rates are associated with QBO modulation of both temperature and constituent fields (mainly ozone). Largest QBO variations in both $\overline{Q}$ and $\overline{w^*}$ are observed in the upper stratosphere (near 40 km). The temperature and ozone contributions to radiative heating are in phase in the upper stratosphere, but their effects tend to cancel in the lower stratosphere. The magnitude of interannual variations in $\overline{w^*}$ is relatively small compared to background seasonal variations, and the partial cancellation of temperature and ozone radiative effects in the lower stratosphere may contribute to uncertainties in calculation of these small values. There is a linear relationship observed between $\overline{w^*}$ and $\overline{u}_z$ in the Tropics due to the correlation of both of these quantities with temperature. This empirical result can allow simple estimation of $\overline{w^*}$ anomalies from $\overline{u}_z$ measurements (such as from Singapore winds). Note the underestimate of maximum $\overline{u}_z$ in the UKMO data (discussed above) implies a similar 30%–50% underestimate of maximum $\overline{w^*}$ values derived here.

Extratropical QBO anomalies in $\overline{w^*}$ show midlatitude maxima nearly identical (but oppositely signed) to temperature anomalies; this is due to the dependence of $\overline{Q}$ on temperature. These midlatitude QBO $\overline{w^*}$ anomalies

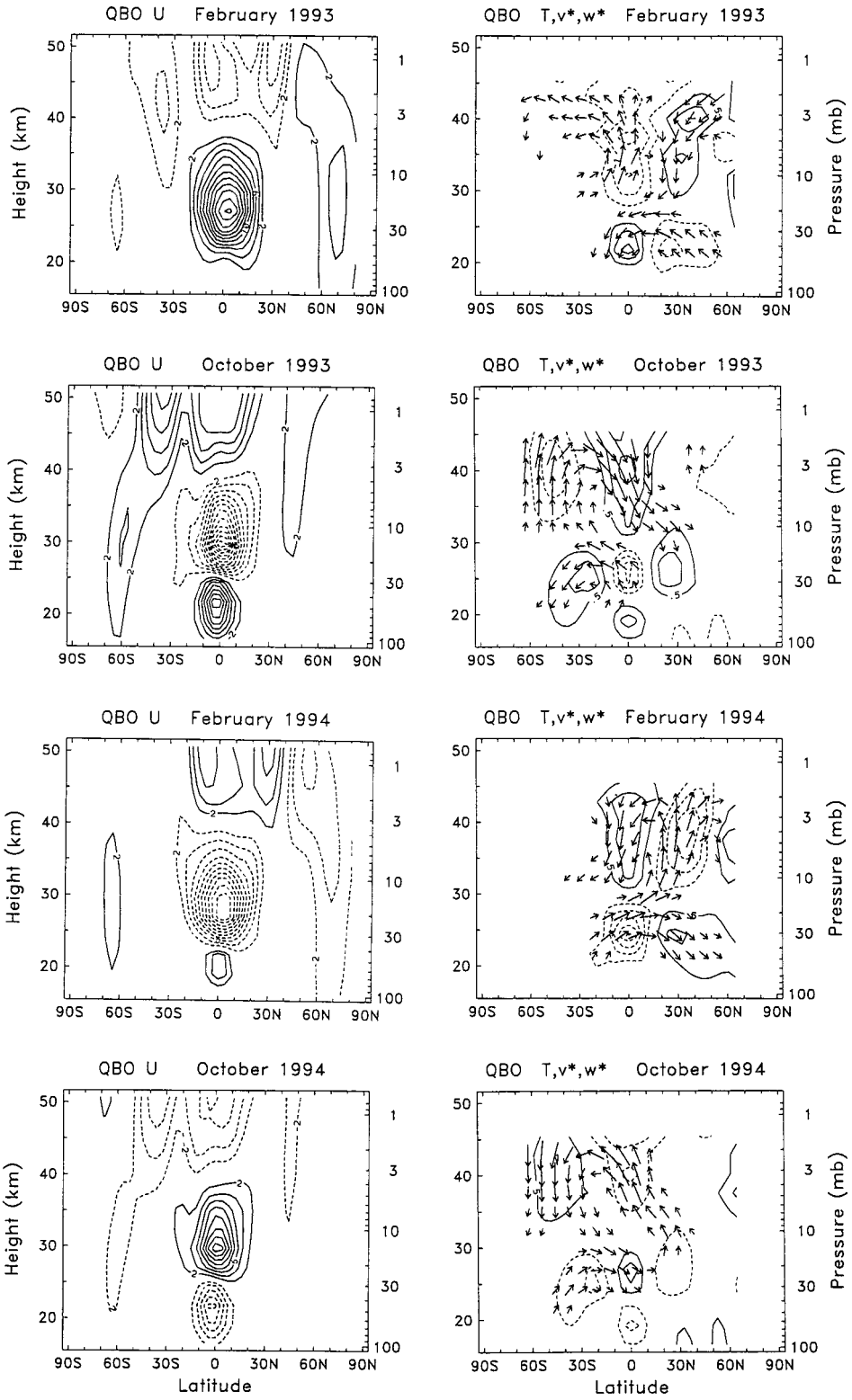

FIG. 18. Cross sections of QBO anomalies through one complete cycle during 1993–94. (left) Zonal wind anomalies, with contour interval of 2 m s^{-1} (zero contours omitted), and (right) temperature anomalies as contours (± 0.5, 1.0, 1.5, $\cdots$ K) and components of the residual mean circulation $(\overline{v^*}, \overline{w^*})$ as vectors (scaled by an arbitrary function of altitude).

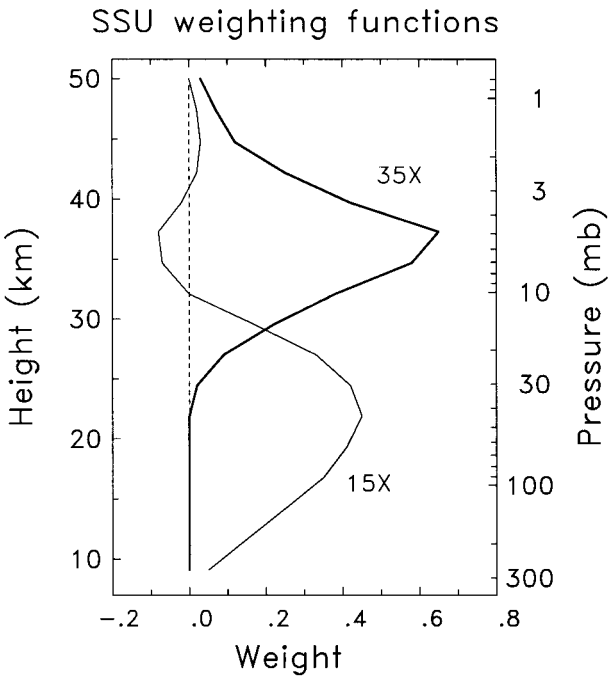

FIG. 19. Weighting functions for SSU channels 15*X* and 35*X*.

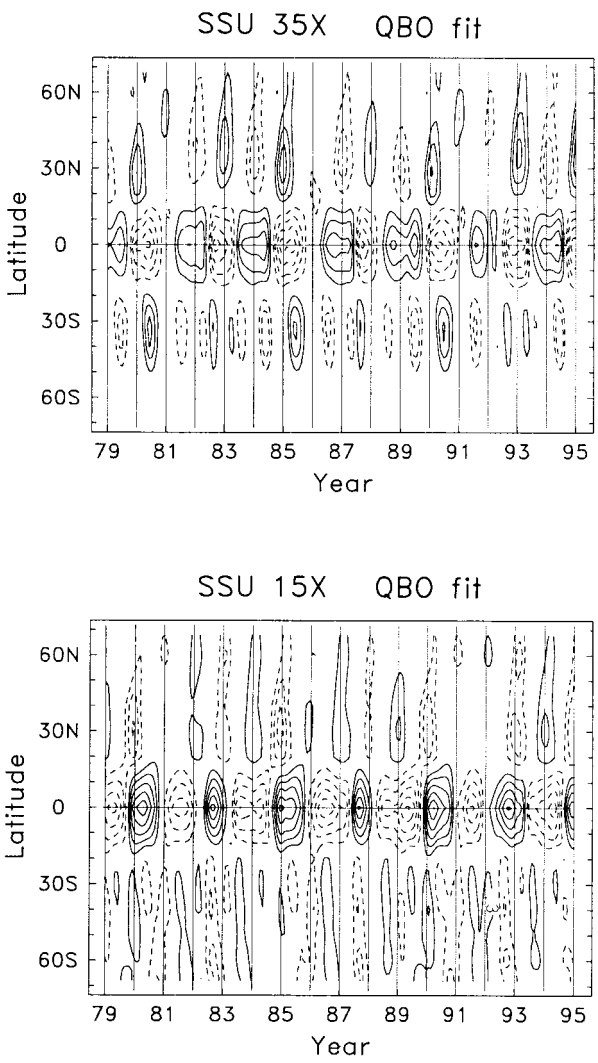

FIG. 20. Latitude–time diagrams of satellite brightness temperature anomalies associated with the QBO, spanning 1979–1994. (Top) from SSU channel 35*X* (spanning ~32–42 km) and (lower) from channel 15*X* (~15–25 km); the weighting functions for these channels are shown in Fig. 19. Contour interval is 0.3 K, with zero contours omitted. Note the vertical out-of-phase structure in both Tropics and midlatitudes.

exhibit out of phase vertical structure between the lower and upper stratosphere, and strong seasonal synchronization, echoing the temperature anomalies. The temperature and circulation patterns in the meridional plane (Fig. 18) are similar in some respects to those anticipated theoretically for the QBO (Plumb and Bell 1982), particularly the symmetric patterns in the lower stratosphere during September 1993 and 1994 seen in Fig. 18. However, the midlatitude patterns in NH winter and in the SH upper stratosphere are highly asymmetric and exhibit wider meridional scale than the QBO circulation in such idealized models. The long-term three-dimensional simulation of Hamilton (1998) does exhibit asymmetric patterns in NH winter similar to those shown here. Explanations for this asymmetry have been proposed as being due to coupling of the QBO and seasonal cycles via seasonality in the stratospheric meridional circulation (Holton 1989; Gray and Dunkerton 1990) and modulation of winter hemisphere planetary wave driving (O'Sullivan and Salby 1990; O'Sullivan and Young 1992; Tung and Yang 1994b). Jones et al. (1998) and Kinnersley (1999) have recently provided a simple explanation of this seasonal coupling as a result of nonlinear momentum advection in the Tropics and subtropics (the background seasonal $\overline{v}^*$ circulation advects the QBO wind anomalies into the winter hemisphere). One aspect of the coupling between the QBO and the seasonal cycle is that the phase relationship is continually changing [due to the ~28 month period of the QBO; see Gray and Dunkerton (1990)]. Thus the details of the QBO patterns in extratropics will likely slowly evolve in time; for this short record somewhat more coherent extratropical signals are observed in the NH. Details of the tropical–midlatitude coupling associated with the QBO is an intriguing problem that invites further analyses.

Acknowledgments. A significant fraction of this work was completed while WJR was on sabbatical leave at the Cooperative Research Center for Southern Hemisphere Meteorology at Monash University in Melbourne, Australia. The authors thank Barbara Naujokat from the Free University of Berlin for Singapore zonal winds and David Cullum from the UKMO Hadley Cen-

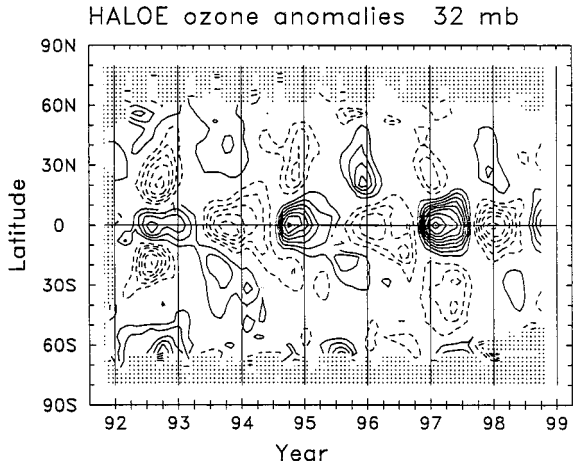

FIG. 21. Latitude–time diagram of interannual anomalies in ozone at 32 mb, derived from HALOE data. Contour interval is 0.1 ppmv, with zero contours omitted. Shaded polar regions denote missing data.

tre for Singapore temperature data. Rolando Garcia and Anne Smith provided constructive reviews. Marilena Stone expertly prepared the manuscript. This work was partly sponsored under NASA Grants W-18181 and W-16215. NCAR is sponsored by the National Science Foundation.

REFERENCES

Andrews, D. G., J. R. Holton, and C. B. Leovy, 1987: *Middle Atmosphere Dynamics.* Academic Press, 489 pp.

Angell, J. K., 1993: Comparison of stratospheric warming following Agung, El Chichón and Pinatubo volcanic eruptions. *Geophys. Res. Lett.,* **20,** 715–718.

——, and J. Korshover, 1962: The biennial wind and temperature oscillation of the equatorial stratosphere and their possible extension to higher latitudes. *Mon. Wea. Rev.,* **90,** 127–132.

Baldwin, M. P., and T. J. Dunkerton, 1991: Quasi-biennial oscillation above 10 mb. *Geophys. Res. Lett.,* **18,** 1205–1208.

——, and K. K. Tung, 1994: Extratropical QBO signals in angular momentum and wave forcing. *Geophys. Res. Lett.,* **21,** 2717–2720.

Bowman, K. P., 1989: Global patterns of the quasi-biennial oscillation in total ozone. *J. Atmos. Sci.,* **46,** 3382–3343.

Christy, J. R., and S. J. Drouilhet Jr., 1994: Variability in daily, zonal mean lower-stratospheric temperatures. *J. Climate,* **7,** 106–120.

Dunkerton, T. J., and D. P. Delisi, 1985: Climatology of the equatorial lower stratosphere. *J. Atmos. Sci.,* **42,** 376–396.

——, and M. P. Baldwin, 1992: Modes of interannual variability in the stratosphere. *Geophys. Res. Lett.,* **19,** 49–52.

Eluszkiewicz, J., and Coauthors, 1996: Residual circulation in the stratosphere and lower mesosphere as diagnosed from microwave limb sounder data. *J. Atmos. Sci.,* **53,** 217–240.

——, D. Crisp, R. G. Grainger, A. Lambert, A. E. Roche, J. B. Kumer, and J. L. Mergenthaler, 1997: Sensitivity of the residual circulation diagnosed from UARS data to the uncertainties in the input fields and to the inclusion of aerosols. *J. Atmos. Sci.,* **54,** 1739–1757.

Fleming, E. L., and S. Chandra, 1989: Equatorial zonal wind in the middle atmosphere derived from geopotential weight and temperature data. *J. Atmos. Sci.,* **46,** 860–866.

Gille, J. C., and L. V. Lyjak, 1986: Radiative heating and cooling rates in the middle atmosphere. *J. Atmos. Sci.,* **43,** 2215–2229.

——, ——, and A. K. Smith, 1987: The global mean residual circulation in the middle atmosphere for the northern winter period. *J. Atmos. Sci.,* **44,** 1437–1452.

Gray, L. J., and T. J. Dunkerton, 1990: The role of the seasonal cycle in the quasi-biennial oscillation of ozone. *J. Atmos. Sci.,* **47,** 2429–2451.

Hamilton, K., 1984: Mean wind evolution through the quasi-biennial cycle in the tropical lower stratosphere. *J. Atmos. Sci.,* **41,** 2113–2125.

——, 1998: Effects of an imposed quasi-biennial oscillation in a comprehensive troposphere-stratosphere-mesosphere general circulation model. *J. Atmos. Sci.,* **55,** 2393–2418.

Hasebe, F., 1994: Quasi-biennial oscillations of ozone and diabatic circulation in the equatorial stratosphere. *J. Atmos. Sci.,* **51,** 729–745.

Hollandsworth, S. M., K. P. Bowman, and R. D. McPeters, 1995: Observational study of the quasi-biennial oscillation in ozone. *J. Geophys. Res.,* **100,** 7347–7361.

Holton, J. R., 1989: Influence of the annual cycle in meridional transport on the quasi-biennial oscillation in total ozone. *J. Atmos. Sci.,* **46,** 1434–1439.

——, and H. C. Tan, 1980: The influence of the equatorial quasi-biennial oscillation on the global circulation at 50 mb. *J. Atmos. Sci.,* **37,** 2200–2208.

——, and ——, 1982: The quasi-biennial oscillation in the Northern Hemisphere lower stratosphere. *J. Meteor. Soc. Japan,* **60,** 140–148.

Huang, T., 1996: The impact of solar radiation on the quasi-biennial oscillation of ozone in the tropical stratosphere. *Geophys. Res. Lett.,* **23,** 3211–3214.

Jones, D. B., H. R. Schneider, and M. B. McElroy, 1998: Effects of the quasi-biennial oscillation on the zonally averaged transport of tracers. *J. Geophys. Res.,* **103,** 11 235–11 249.

Kinnersley, J. S., 1999: Seasonal asymmetry of the low- and middle-latitude QBO circulation anomaly. *J. Atmos. Sci.,* in press.

Labitzke, K., and M. P. McCormick, 1992: Stratospheric temperature increases due to Pinatubo aerosols. *Geophys. Res. Lett.,* **19,** 207–210.

Nash, J., 1988: Extension of explicit radiance observations by the stratospheric sound unit into the lower stratosphere and lower mesosphere. *Quart. J. Roy. Meteor. Soc.,* **114,** 1153–1171.

Naujokat, B., 1986: An update of the observed quasi-biennial oscillation of the stratospheric winds over the Tropics. *J. Atmos. Sci.,* **43,** 1873–1877.

Olaguer, E. P., H. Yang, and K. K. Tung, 1992: A reexamination of the radiative balance of the stratosphere. *J. Atmos. Sci.,* **49,** 1242–1263.

Ortland, D. A., W. R. Skinner, P. B. Hays, M. D. Burrage, R. S. Lieberman, A. R. Marshall, and D. A. Gell, 1996: Measurements of stratospheric winds by the high resolution Doppler imager. *J. Geophys. Res.,* **101,** 10 351–10 363.

O'Sullivan, D., and M. Salby, 1990: Coupling of the quasi-biennial oscillation and extratropical circulation in the stratosphere through planetary wave transport. *J. Atmos. Sci.,* **47,** 650–673.

——, and R. E. Young, 1992: Modeling the quasi-biennial oscillation's effect on the winter stratospheric circulation. *J. Atmos. Sci.,* **49,** 2437–2448.

——, and T. J. Dunkerton, 1994: Seasonal development of the extratropical QBO in a numerical model of the middle atmosphere. *J. Atmos. Sci.,* **51,** 3706–3721.

Pawson, S., and M. Fiorino, 1998: A comparison of reanalyses in the tropical stratosphere. Part 2: The quasi-biennial oscillation. *Climate Dyn.,* **14,** 645–658.

Plumb, R. A., and R. C. Bell, 1982: A model of the quasi-biennial oscillation on an equatorial beta-plane. *Quart. J. Roy. Meteor. Soc.,* **108,** 335–352.

Randel, W. J., and J. B. Cobb, 1994: Coherent variations of monthly mean column ozone and lower stratospheric temperature. *J. Geophys. Res.,* **99,** 5433–5447.

——, and F. Wu, 1996: Isolation of the ozone QBO in SAGE II data by singular value decomposition. *J. Atmos. Sci.,* **53,** 2546–2559.
Reed, R. J., W. J. Campbell, L. A. Rasmussen, and D. G. Rodgers, 1961: Evidence of downward-propagating annual wind reversal in the equatorial stratosphere. *J. Geophys. Res.,* **66,** 813–818.
Rosenlof, K. H., 1995: Seasonal cycle of the residual mean meridional circulation in the stratosphere. *J. Geophys. Res.,* **100,** 5173–5191.
Russell, J. M., III, and Coauthors, 1993: The halogen occultation experiment. *J. Geophys. Res.,* **98,** 10 777–10 797.
Swinbank, R., and A. O'Neill, 1994a: A stratosphere–troposphere assimilation system. *Mon. Wea. Rev.,* **122,** 686–702.
——, and ——, 1994b: Quasi-biennial and semi-annual oscillations in equatorial windfields constructed by data assimilation. *Geophys. Res. Lett.,* **21,** 2099–2102.
Tucker, G. B., and J. M. Hopwood, 1968: The 26-month zonal wind oscillation in the lower stratosphere of the Southern Hemisphere. *J. Atmos. Sci.,* **25,** 293–298.
Tung, K. K., and H. Yang, 1994a: Global QBO in circulation and ozone. Part I: Reexamination of observational evidence. *J. Atmos. Sci.,* **51,** 2699–2707.
——, and ——, 1994b: Global QBO in circulation and ozone. Part II: A simple mechanistic model. *J. Atmos. Sci.,* **51,** 2708–2721.
Veryard, R. G., and R. A. Ebdon, 1961: Fluctuations in tropical stratospheric winds. *Meteor. Mag.,* **90,** 125–143.
Wallace, J. M., R. Panetta, and J. Estberg, 1993: Representation of the equatorial quasi-biennial oscillation in EOF phase space. *J. Atmos. Sci.,* **50,** 1751–1762.
Weaver, C. J., A. R. Douglass, and R. B. Rood, 1993: Thermodynamic balance of three-dimensional stratospheric winds derived from a data assimilation procedure. *J. Atmos. Sci.,* **50,** 2987–2993.
Zawodny, J. M., and M. P. McCormick, 1991: Stratospheric Aerosol and Gas Experiment II measurements of the quasi-biennial oscillation in ozone and nitrogen dioxide. *J. Geophys. Res.,* **96,** 9371–9377.